Contribution of Incoherent Effects to Bremsstrahlung of Fast Particles in Crystals

V. V. Syshchenko[a], A. I. Tarnovskii[a], and N. F. Shul'ga[b]

[a] *Belgorod State University, Belgorod, 308015 Russia*

e-mail: syshch@bsu.edu.ru

[b] *Akhiezer Institute for Theoretical Physics, Kharkiv Institute of Physics and Technology National Science Center, Kharkiv, 61108 Ukraine*

Abstract—Incoherent radiation of high-energy electrons in crystals is due to the thermal spread of atoms about their equilibrium positions in lattices. The procedure for modeling incoherent radiation developed previously makes it possible to interpret some results of recent experiments conducted on the Mainz microtron (abbreviated MAMI).

INTRODUCTION

The cross section for bremsstrahlung of relativistic electrons in crystals [1–3] is the sum of the coherent term (which is due to the periodicity of the spatial arrangement of atoms in lattices) and the incoherent term (which is due to the thermal spread of atomic positions about the lattice sites). In this case, the interference of radiation produced during interaction of particles with different atomic crystals chains and planes leads to the considerable dependence of the intensity of coherent radiation on the crystal orientation with respect to the beam of projectiles. On the other hand, the incoherent radiation spectrum is similar to the Bethe–Heitler radiation spectrum in an amorphous medium and, at first glance, the intensity of the incoherent portion of bremsstrahlung must be independent of the crystal orientation. However, it was shown in [4–6] that the redistribution of the flux density of particles in crystals related to the channeling effect [2, 3, 7–9] can lead to the appearance of a considerable orientation dependence of the intensity of incoherent radiation. The procedure for modeling incoherent radiation developed in [4–6] made it possible to interpret orientational effects observed in previous experiments conducted at the Kharkiv Institute of Physics and Technology [10]. In the present paper, our procedure is applied to the analysis of recent experimental data obtained at the microtron MAMI operating at Mainz University [11].

PROCEDURE

The process of bremsstrahlung of relativistic electrons is developed in a large space region along the particle momentum; it is called the coherence length $l_{\rm coh} \sim 2\varepsilon\varepsilon'/m^2c^3\omega$, where ε is the energy of the initial electron, ω is the frequency of a radiated photon, $\varepsilon' = \varepsilon - \hbar\omega$, m is the electron mass, and c is the light velocity in vacuum [1, 2]. In a broad range of radiation frequencies, the coherence length exceeds the interatomic distances in materials,

$$l_{\rm coh} \gg a. \tag{1}$$

In this case, the effective constant of the lattice-atom–electron interaction can be larger than unity, which makes it possible to use the quasiclassical approximation in order to describe electron radiation in crystals. In this case, for the frequency range that is interesting to us and satisfies condition (1), the spectral density of bremsstrahlung is described by the dipole formula [2]:

$$\frac{d\mathrm{E}}{d\omega} = \frac{e^2\omega}{2\pi c^2} \times \int_{\delta}^{\infty} \frac{dq}{q^2}\left[1 + \frac{(\hbar\omega)^2}{2\varepsilon\varepsilon'} - 2\frac{\delta}{q}\left(1 - \frac{\delta}{q}\right)\right]\left|\sum_n \vartheta_n \exp\left(icqt_n\right)\right|^2, \tag{2}$$

where $\delta = m^2c^3\omega/2\varepsilon\varepsilon' \sim l_{\rm coh}^{-1}$, ϑ_n is the two-dimensional angle of electron scattering during the collision with the nth atom of the medium, and t_n is the instant of collision.

The angle of scattering by the atom as a function of the collision impact parameter can be easily found from the equation of electron motion in the transverse plane [2, 9]:

$$\dot{\mathbf{v}}_\perp = -\frac{c^2 e}{\varepsilon}\frac{\partial}{\partial\boldsymbol{\rho}}U(\mathbf{r}). \tag{3}$$

Choosing the atomic potential in the form of the screened Coulomb potential $U(r) = (Z|e|/r)\exp(-r/R)$, where Z is the atomic number, we find

$$\vartheta(\boldsymbol{\rho}_n) = \frac{2Ze|e|}{\varepsilon R} K_1\left(\frac{\rho_n}{R}\right)\frac{\boldsymbol{\rho}_n}{\rho_n}, \quad (4)$$

where $K_1(x)$ is the third-kind modified Bessel function (the Macdonald function) and $\boldsymbol{\rho}_n$ is the impact parameter of the nth collision.

Formula (2) describes the radiation intensity of a separate electron moving along a given trajectory. The radiation of the uniform beam of particles of the unit density is characterized by the radiation intensity equal to intensity (2) integrated over the impact parameters of particle incidence on the target:

$$\frac{dK}{d\omega} = \int \frac{d\mathrm{E}}{d\omega} d^2\rho_0. \quad (5)$$

In particular, for radiation in the field of the separate atom, using (4) leads to the Bethe–Heitler formula

$$\frac{dK}{d\omega} = \hbar\omega\frac{d\sigma_{\mathrm{BH}}}{d\omega} = \frac{16}{3}\frac{Z^2e^6}{m^2c^5}\frac{\varepsilon'}{\varepsilon}\left(1+\frac{3}{4}\frac{(\hbar\omega)^2}{\varepsilon\varepsilon'}\right)\ln\left(\frac{mRc}{\hbar}\right). \quad (6)$$

(with logarithmic accuracy caused by the inapplicability of the dipole approximation at impact distances that are less than $\hbar/mc$).

We now consider radiation produced during electron incidence on the crystal at the small angle ψ made with one of the crystallographic axes densely packed with atoms (the z axis). In this case, correlations between successive collisions with atoms lead to the appearance of coherent effects in radiation [1, 2]. The averaging of the quantity $\left|\sum_n \vartheta_n \exp(icqt_n)\right|^2$ in (2) over thermal oscillations of atoms in crystals leads to the decomposition of this quantity (and the radiation intensity) into two added terms describing coherent and incoherent effects in radiation:

$$\left\langle \left| \sum_n \vartheta_n \exp(icqt_n) \right|^2 \right\rangle = \sum_{n,m} \exp[iqc(t_n - t_m)]\langle\vartheta(\boldsymbol{\rho}_n + \mathbf{u}_n)\rangle\langle\vartheta(\boldsymbol{\rho}_m + \mathbf{u}_m)\rangle \quad (7)$$
$$+ \sum_n \left\{ \left\langle (\vartheta(\boldsymbol{\rho}_n + \mathbf{u}_n))^2 \right\rangle - (\langle\vartheta(\boldsymbol{\rho}_n + \mathbf{u}_n)\rangle)^2 \right\},$$

where $\boldsymbol{\rho}_n = \boldsymbol{\rho}(t_n) - \boldsymbol{\rho}_n^0$ is the impact parameter of the collision with the nth atom in its equilibrium position $\boldsymbol{\rho}_n^0$; $\boldsymbol{\rho}(t)$ is the electron trajectory in the plane orthogonal to the z axis, and $\mathbf{u}_n$ is the thermal displacement of the nth atom with respect to its equilibrium position.

Coherent effects in the radiation process were studied in many theoretical and experimental papers [1–3]; however, we concentrate our attention on the second term in (7) describing incoherent radiation. Substituting formula (4) for the angle of scattering by the separate atom to the second term in (7) leads to the following expression for the incoherent part:

$$\left(\frac{d\mathrm{E}}{d\omega}\right)_{\mathrm{incoh}} = \frac{8}{3\pi}\frac{Z^2e^6}{m^2R^2c^5}\frac{\varepsilon'}{\varepsilon}\left(1+\frac{3}{4}\frac{(\hbar\omega)^2}{\varepsilon\varepsilon'}\right)\sum_n F(\boldsymbol{\rho}_n), \quad (8)$$

where

$$F(\boldsymbol{\rho}) = \left\langle \left(K_1\left(\frac{|\boldsymbol{\rho}+\mathbf{u}|}{R}\right)\right)^2\right\rangle - \left\langle \frac{\boldsymbol{\rho}+\mathbf{u}}{|\boldsymbol{\rho}+\mathbf{u}|} K_1\left(\frac{|\boldsymbol{\rho}+\mathbf{u}|}{R}\right)\right\rangle^2.$$

It is convenient to compare the effectiveness of incoherent radiation in the crystal (which is of interest to us) with that of radiation in the amorphous medium (for the equal number N of collisions with atoms). It is easy to see that the ratio of these two quantities is

$$N_\gamma = \frac{\int d^2\rho_0 \left(\frac{d\mathrm{E}}{d\omega}\right)_{\mathrm{incoh}}}{N\hbar\omega\frac{d\sigma_{\mathrm{BH}}}{d\omega}} = \frac{\int d^2\rho_0 \sum_n F(\boldsymbol{\rho}_n)}{2\pi N R^2 \ln\left(\frac{mRc}{\hbar}\right)}, \quad (9)$$

where integration over $d^2\rho_0$ means integration over all possible points of electron entry into the crystal within the limits of one unit cell.

The impact parameters $\boldsymbol{\rho}_n$ for collisions with the atoms are determined using the electron trajectory in the crystal found by the numerical modeling, which was discussed in detail in [4–6]. The integration over $d^2\rho_0$ can be performed by the Monte-Carlo method.

Formula (7) for $q = 0$ describes the average squared angle of multiple scattering of particles in crystals. It is easy to see that multiple scattering is also the sum of coherent scattering (which manifested itself as scattering in continuous potentials of atomic chains [2, 7–9]) and incoherent scattering by thermal oscillations of atoms. Substituting (4) in the second term in (7) leads to the formula for the average squared angle of incoherent scattering:

$$\langle\vartheta^2\rangle_{\mathrm{incoh}} = \frac{4Z^2e^4}{\varepsilon^2R^2}\sum_n F(\boldsymbol{\rho}_n). \quad (10)$$

Thus, in the modeling of the electron trajectory in the crystal, the presence of incoherent scattering by thermal oscillations of atoms can be taken into account by adding a random quantity obeying the Gauss distribution with the dispersion $\left(2Z^2e^4c^2/\varepsilon^2R^2\right)F(\boldsymbol{\rho}_n)$ to each of the components of the electron velocity in the xy plane at the instant of collision with the nth atom.

RESULTS AND DISCUSSION

Specific modeling parameters were chosen according to conditions of one of the experiments described in [11]. An integral intensity of radiation with an energy of 15 MeV or more was registered in this experiment. This radiation was produced in the case in

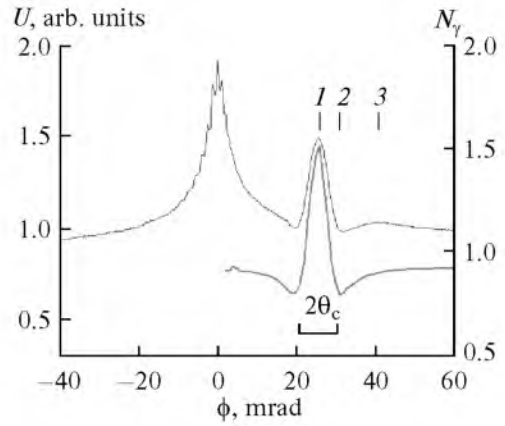

Fig. 1. Integral intensity of radiation with energy of 15 MeV or higher registered at the 855-MeV electron incidence on a thin Si crystal (14.7 μm) at a small angle with the ⟨100⟩ axis under the conditions shown in Fig. 14b in [11] (the upper curve) and the relative effectiveness of incoherent radiation according to the modeling results (the lower curve).

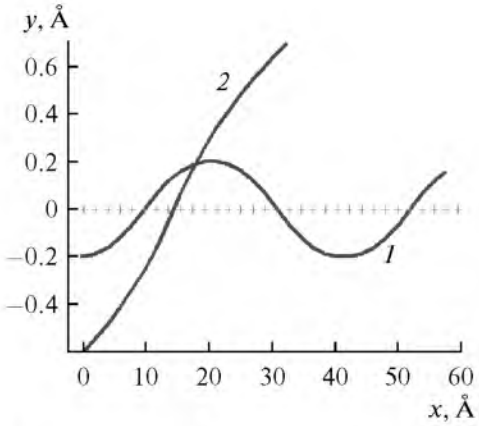

Fig. 2. Projections of the electron trajectories in the crystal on the (100) plane in (*1*) the channeling regime and (*2*) the case of overbarrier motion. Crosses denote the positions of atomic chains parallel to the ⟨100⟩ axis and producing the attracting potential of the $(0\bar{1}1)$ plane. The *x* and *y* axes are parallel to the $\langle 0\bar{1}\bar{1}\rangle$ and $\langle 0\bar{1}1\rangle$ directions, respectively.

which the beam of 855-MeV electrons was incident on the Ge crystal fixed at a goniometer so that the angle ψ of beam incidence with the ⟨100⟩ axis and the angle θ with the $(0\bar{1}1)$ plane turned out to be small. The angles ϕ and θ were varied when the goniometric angle ϕ was scanned; in this case, it turned out that $\psi \approx \phi$ in the angular range shown in Fig. 1 (see Appendix).

Figure 1 shows results of modeling incoherent radiation according to formula (9) together with the experimental data [11]. Because the Bethe–Heitler spectrum is almost planar, the integral intensity of incoherent radiation turns out to be proportional (with a good accuracy) to the relative spectral density of radiation obtained as a result of modeling. It can be seen from comparison of these two curves that the right peak on the experimental curve is due to the orientation dependence of the effectiveness of incoherent radiation in the crystal. (The contribution of coherent effects produced the difference between the modeling results and the experimental curve can be calculated using standard formulas of the theory of coherent bremsstrahlung [2]. Thus, the left peak on the experimental curve is due to the coherent contributions of crystallographic axes with the common ⟨100⟩ axis [11]).

The reason for the appearance of this dependence is as follows. The correlations between the successive collisions of particles with different atomic chains constituting this plane can occur at particle incidence at a small angle on any crystallographic plane densely packed with atoms. The presence of such correlations is manifested in that the particles move in the continuous potentials of atomic planes [2, 7–9]. If the energy $\varepsilon_\perp = \varepsilon\theta^2/2$ of transverse particle motion does not exceed the height of the potential barrier produced by the continuous plane potential, then the particle moves in the plane channeling regime. The electron in the channeling regime moves near the atomic plane (Fig. 2) and experiences, on average, a larger number of collisions with atoms with small impact parameters than in the case of its motion in the amorphous medium. This is the reason for the maximum of the relative effectiveness of incoherent radiation in Fig. 1 observed for the goniometric angle ϕ corresponding to the zero angle θ of electron incidence on the $(0\bar{1}1)$ plane.

As the incidence angle increases, more and more particles move in the over-barrier regime. The over-barrier electron passes rapidly through the atomic plane (Fig. 2) and experiences a smaller number of short-range collisions with atoms than in the case of its motion in the amorphous medium. The minimum of the effectiveness of incoherent radiation is reached at the incidence angle equal to the critical channeling angle θ_c determined from the condition of equality between the transverse motion energy and the height of the potential barrier produced by the continuous potential of the atomic plane. In our case, the critical angle of plane channeling is $\theta_c \approx 2.3 \times 10^{-4}$ rad. It should be mentioned that, for positrons, the case is opposite, namely, the minimum of the effectiveness in the case of channeling and the maximum for $\theta = \theta_c$ [4, 5].

For incidence angles greatly exceeding the critical channeling angle, the particle trajectory becomes close to the rectilinear one, the collisions with atoms with all possible impact parameters become equiprobable as in the amorphous medium, and the effectiveness of incoherent radiation in the crystal tends to the Bethe–Heitler limit (up to the Debye–Waller factor).

Incoherent scattering of electrons by thermal oscillations of atoms weakens the above-mentioned typical

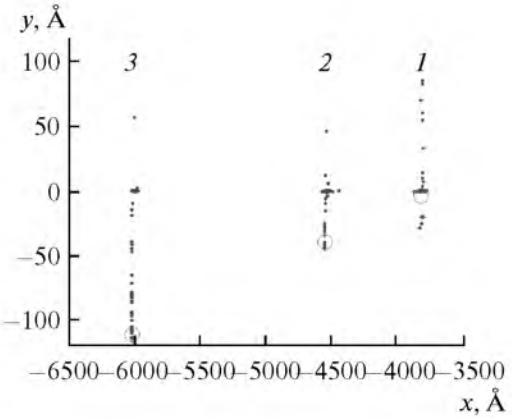

Fig. 3. Distribution of the electrons over the coordinates at the crystal output. The points of particle entry into the crystal are distributed randomly within the limits of the unit cell with the center at the origin of coordinates. Circles denote the regions of electron departure in the case of their rectilinear motion.

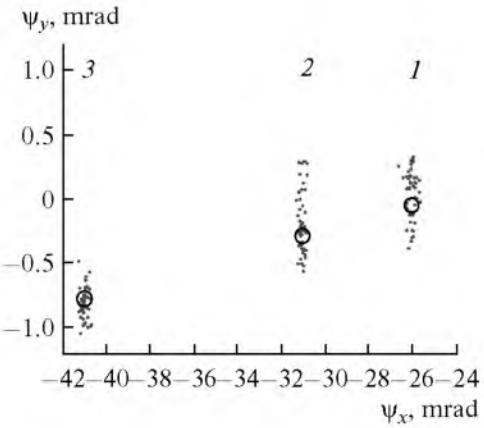

Fig. 4. Distribution of electrons at the crystal output over the directions of motion with respect to the ⟨100⟩ axis.

features slightly: an electron scattered at a large angle can leave the channel (to be dechanneled) or, conversely, return to the channel (to be rechanneled).

The described changes in the character of particle motion in the crystal are presented in Fig. 3, which shows the results of modeling the coordinates of electrons at the crystal output. Three groups of points correspond to three different crystal orientations with respect to the beam that are shown in Fig. 1. In all cases, electrons enter the crystal within the limits of the unit cell located at the origin of coordinates. The circles denote the regions of electron exit in the case of their rectilinear motion. It can be seen that the portion of channeled electrons decreases successively in cases 1, 2, and 3.

Figure 4 shows results of modeling the directions of electron exit from the crystal under the same conditions as in Fig. 3 (the components of the two-dimensional angle made by the direction of electron motion with the <100> axis are equal to the corresponding components of the electron velocity divided by c: $\psi_x = v_x/c$ and $\psi_y = v_y/c$). It can be seen that, in case 3, the directions of motion of all electrons at the crystal output are concentrated near the initial direction of the beam. The above-mentioned fact that the particle trajectories in the crystal differ slightly from the rectilinear ones for $\theta \gg \theta_c$ is manifested in this.

Thus, the modeling results show a considerable dependence of the incoherent bremsstrahlung yield on the crystal orientation with respect to the beam of incident particles at incidence angles that are close to the critical angle of plane channeling. This orientation dependence is due to special features of the dynamics of charged particles in crystals. As showed the comparison with the experimental data, the contribution of incoherent mechanisms to the radiation process can considerably exceed the quantity determined using the Bethe–Heitler formula under certain conditions. The modeling results make it possible to interpret the data of the experiment in [11], in which the orientation dependence of the integral intensity of fast electron radiation in crystals was measured.

CONCLUSIONS

Our results show that taking into account incoherent effects produced during interaction of high-energy particles with regular structures (crystals) is important. Our developed approach can be used to plan experiments and analyze their results, as well as in the fabrication of new radiation sources.

APPENDIX

In the experiment in [11], the Si crystal was fixed at a three-axis goniometer as is shown in Fig. 5. The beam of electrons was incident on the crystal in the positive direction of the X axis of the laboratory X, Y, Z system of coordinates. The axes of the moving coordinate system corresponded to the ⟨100⟩, ⟨010⟩, and ⟨001⟩ axes of the Si crystal. We show how the angles of crystal rotation about the goniometer axes ϕ, Θ, and α are related to the angles ψ and θ, which are interesting to us.

The angles Θ and α remain fixed ($\Theta \approx 1.2 \times 10^{-3}$ and $\alpha \approx -\pi/4 + 0.049$ rad) and the angle ϕ is varied from −0.04 to 0.06 rad in the discussed experiment. It is easy to show that, in this range of parameters, the angle ψ between the beam direction and the ⟨100⟩ axis is determined by the relation

$$\cos\psi = \cos\Theta\cos\phi,$$

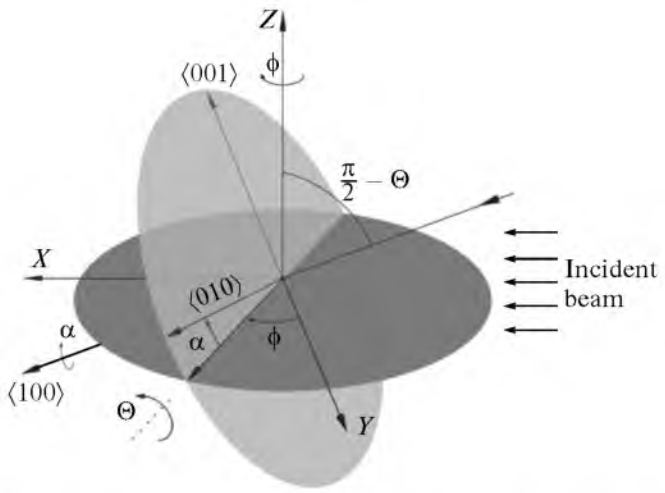

Fig. 5. Orientation of the Si crystal at the goniometer with respect to the beam in the experiment in [11].

and the angle θ between the beam direction and the $(0\bar{1}1)$ plane is determined by the relation

$$\sin\theta = \frac{1}{\sqrt{2}}(\cos\phi\cos\alpha\sin\Theta - \cos\phi\sin\alpha\sin\Theta - \sin\phi\cos\alpha - \sin\phi\sin\alpha).$$

In the angular range near the discussed maximum of the radiation intensity, we can approximately write

$$\psi \approx \phi, \quad \theta \approx \Theta - \left(\alpha + \frac{\pi}{4}\right)\phi.$$

ACKNOWLEDGMENTS

This work was supported by a grant of Belgorod State University.

REFERENCES

1. M. L. Ter-Mikaelyan, *The Influence of the Medium on High-Energy Electromagnetic Processes* (Izd-vo AN Arm.SSR, Yerevan, 1969) [in Russian].
2. A. I. Akhiezer and N. F. Shul'ga, *High Energy Electrodynamics in Matter* (Nauka, Moscow, 1993) [in Russian].
3. U. I. Uggerhoj, Rev. Mod. Phys. **77**, 1131 (2005).
4. N. F. Shul'ga and V. V. Syshchenko, Nucl. Instrum. Methods Phys. Res. B **227**, 125 (2005).
5. V. V. Syshchenko, A. I. Tarnovskii, and N. F. Shul'ga, Poverkhnost', No. 4, 80 (2008) [J. Surf. Invest. **2**, 321 (2008)].
6. V. V. Syshchenko, A. I. Tarnovskii, and N. F. Shul'ga, Poverkhnost', No. 3, 68 (2009).
7. J. Lindhard, Dan. Vid. Selsk. Mat. Phys. Medd. **34**, 30 (1965).
8. D. S. Gemmell, Rev. Mod. Phys **46**, 129 (1974).
9. A. I. Akhiezer, N. F. Shul'ga, V. I. Truten', et al., Usp. Fiz. Nauk **165** (10), 1165 (1995) [Phys. Usp. **38**, 1119 (1995)].
10. V. M. Sanin, V. M. Khvastunov, V. F. Boldyshev, and N. F. Shul'ga, Nucl. Instrum. Methods Phys. Res. B **67**, 251 (1992).
11. H. Backe, P. Kunz, W. Lauth, and A. Rueda, Nucl. Instrum. Methods Phys. Res. B **266**, 3835 (2008).